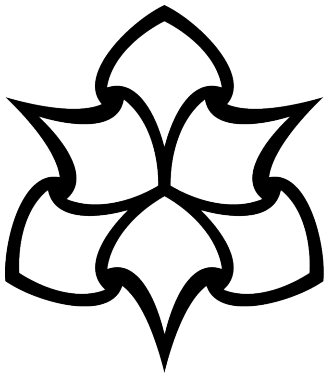

Chemical Engineering Journal 381 (2020) 122343

Contents lists available at ScienceDirect

Chemical Engineering Journal

journal homepage: www.elsevier.com/locate/cej

Additively manufactured graphitic electrochemical sensing platforms

Christopher W. Foster[a,*], Hadil M. Elbardisy[a,b], Michael P. Down[a], Edmund M. Keefe[a], Graham C. Smith[c], Craig E. Banks[a,*]

[a] Faculty of Science and Engineering, Manchester Metropolitan University, Chester Street, Manchester M15 GD, UK
[b] Pharmaceutical Analysis Department, Faculty of Pharmacy, Damanhour University, Damanhour 22511, Egypt
[c] Faculty of Science and Engineering, Department of Natural Sciences, University of Chester, Thornton Science Park, Pool Lane, Ince, Chester CH2 4NU, UK

HIGHLIGHTS

- 3D printing of a range of in-house fabricated graphite/PLA filaments.
- Proof-of-concept shown with the simultaneous detection of lead(II) and cadmium(II).
- Benchmarked electrochemical characterisation and analysis.

ARTICLE INFO

Keywords:
Additive manufacturing (AM)
3D printing
AM sensors
Electroanalytical sensors
3D sensors

ABSTRACT

Additive manufacturing (AM)/3D printing technology provides a novel platform for the rapid prototyping of low cost 3D platforms. Herein, we report for the first time, the fabrication, characterisation (physicochemical and electrochemical) and application (electrochemical sensing) of bespoke nanographite (NG)-loaded (25 wt%) AM printable (*via* fused deposition modelling) NG/PLA filaments. We have optimised and tailored a variety of NG-loaded filaments and their AM counterparts in order to achieve optimal printability and electrochemical behaviour. Two AM platforms, namely AM macroelectrodes (AMEs) and AM 3D honeycomb (macroporous) structures are benchmarked against a range of redox probes and the simultaneous detection of lead (II) and cadmium (II). This proof-of-concept demonstrates the impact that AM can have within the area of electroanalytical sensors.

1. Introduction

Over recent years, the popularity of additive manufacturing (AM) / 3D printing technology has increased significantly due to its ability to provide a unique approach for the rapid prototyping of low cost 3D electrochemical platforms within an array of applications such as energy storage [1], electrosynthesis [2] and electroanalytical studies [3–4]. For example, Tan *et al.* [5] utilised helical-shaped electrodes, AM *via* a selective laser melting (SLM) methodology to produce metallic printed structures for the analytical determination of nitroaromatic compounds and explored towards the sensing of DNA. However, these platforms typically do not provide cost effective electrochemical devices.

The most popular AM technique is *via* fused deposition modelling (FDM), which offers a low cost option for the AM of thermoplastic filaments to create complex three-dimensional structures. Nonetheless, these thermoplastics have to be modified with a sufficient level of active material for them to be useful in the fabrication of electrochemical devices, but this can affect the printability of these AM filaments. This has been reported by Silva *et al.* [6] who investigated the electrochemical performance of graphite-loaded PLA composite, suggesting that levels of over 50 wt% offer the sufficient percolation and conductivity for electrochemical investigations. However, this was not able to be AM to produce electrochemical devices – instead a thick film was produced. Additionally, a report by Wei *et al.* [7] fabricated AM graphitic-based polylactic acid (PLA) and acrylonitrile–butadienestyrene (ABS) conductive filaments with graphene loadings of up to 5.6 wt%, we note that they report that loadings above 7.4 wt% caused significant AM printability issues. Thus, it is evident that the need for highly-loaded AM printable filaments is paramount for the development of AM printed electrochemical devices, but yet can be additively manufactured in a reproducible manner. Recently we have examined a commercially available graphene containing poly(lactic) acid (PLA) filament that could be successfully AM/3D printed into

* Corresponding authors.
E-mail addresses: chris.w.foster@mmu.ac.uk (C.W. Foster), c.banks@mmu.ac.uk (C.E. Banks).

https://doi.org/10.1016/j.cej.2019.122343
Received 26 April 2019; Received in revised form 15 July 2019; Accepted 25 July 2019
Available online 26 July 2019

useful electrochemical geometries [1]. Additionally, Dos Santos *et al.* [8] reported on the utilisation of a commercially available filament to produce additively manufactured electrodes for the electroanalytical detection of dopamine [8]. However in both these cases [1,8], this filament again *only* possessed a very low ~8 wt% active material, which significantly limits its functionality within electrochemical applications.

Herein, we report the fabrication, characterisation (physicochemical and electrochemical) and implementation (electrochemical sensing) of highly-loaded bespoke additive manufacturable printable nanographite (NG)/PLA filaments. We perform rigorous control experiments to tailor a variety of loaded-filaments (1, 5, 15, 20, 25, 30 and 40 wt% NG) and their AM structures, in terms of printability and electrochemical performance. These highly-loaded AM printable NG/PLA filaments possesses sufficient electrical percolation and printability for their potential utilisation as electroanalytical sensing platforms. Proof-of-concept is demonstrated with the utilisation of two AM platforms, namely AM macroelectrodes (AMEs) and AM 3D honeycomb structures which are explored towards the simultaneous detection of lead (II) and cadmium (II). The use of AM allows the honeycomb structure to be easily and rapidly designed and fabricated which cannot easily be fabricated by other manufacturing processes. AM also allows scale up through the use of print farms. Critically comparisons are made of the sensing performances of AMEs to traditionally used screen-printed counterparts.

2. Results and discussion

We first fabricated a range of NG/PLA filaments containing 1, 5, 15, 20, 25, 30 and 40 wt% NG (as described within the Methods Section) in order to understand and tailor their electrochemical performance and additive manufacturing (AM) printability. The percentage mass (*i.e.* NG loading) was *validated* by thermogravimetric analysis (TGA, see Fig. 1A), indicating that all the NG/PLA filaments confirming the correct *wt.* % loading of NG. Fig. 1B shows the percolation study of each of the NG/PLA filaments, where it was found that *wt.* % loadings over 20 wt% start to demonstrate an effective percolation and therefore offer a greater conductivity. However, in terms of AM printability, it becomes apparent that loadings above 25 wt% are too brittle and could not provide a reproducible AM print, simply due to the lack of thermoplastic binding material (*i.e.* PLA).

Topographical analysis of the AM platforms (fabricated *via* AM are shown in Fig. 1C) were next considered and are presented within Fig. 1D, demonstrating the typical features expected for a modified thermoplastic composite, with areas of graphite percolation and fibrous PLA. Raman spectra of the AM electrodes (AMEs), is presented within Fig. 1E with the G band appearing at 1584 cm^{-1} (graphite), the D band at 1363 cm^{-1}, G' band at ~ 2709 cm^{-1}, indicating that the NG is unchanged after the AM process and is percolated within the PLA thermoplastic. Additionally, it demonstrates that the graphite is not highly defective and possesses a relatively small percentage of oxygen species upon the surface [9]. X-ray photoelectron spectroscopy (XPS) was next performed to characterise the AMEs. Fig. 1F presents the survey spectra of this sample, where it is evident that carbon and oxygen dominate the response. High-resolution scans were made over the C 1s lines and curve-fitted to known reference data for chemically-shifted components (Fig. 1F). Such spectra exhibits a main component at 285.0 eV due to carbon in C-C bonds, a weaker component at approximately 286.9 eV due to carbon in C-O bonds, and a component at approximately 289 eV due to carbon in C(=O)O ester groups. Note that pure PLA would be expected to show three components in the C 1s peak, corresponding to the three chemical environments of the PLA monomer. These would be expected to be of equal intensity. The AMEs exhibit a much higher relative intensity for the C–C component, and a reduction in relative intensity of the C-O bonded component.

Electrochemical characterisation was next considered, firstly using the near-ideal outer-sphere redox probe 1 mM hexaammineruthenium (III) chloride/ 0.1 M KCl [10], which does not show any changes in its electron transfer rates due to varying surface chemistry of the electrode surface is only dependent upon the electrode's electronic structure (Density of States (DOS) and the Fermi level) [10–12]. From inspection of the cyclic voltammograms presented within Fig. 2A it is clear that the AMEs exhibit typical graphitic behaviour, which is also reflected in their calculated heterogeneous electron transfer rate constant, k^0, of 8.12×10^{-3} cm s^{-1}. The inner-sphere electrochemical probe, capsaicin, was next considered. This probe is reported within the literature, to undergo an adsorption process upon graphitic electrodes. The electrochemical response of the AMEs towards capsaicin is shown within Fig. 2B. The first electrochemical oxidation (peak I) occurs at a potential of ~ +0.80 V (*vs.* SCE), where upon the reverse cathodic scan the generated molecule (with an *o*-benzoquinone unit), is reduced at ~ +0.24 V (peak III) to produce an *o*-benzenediol derivative that is

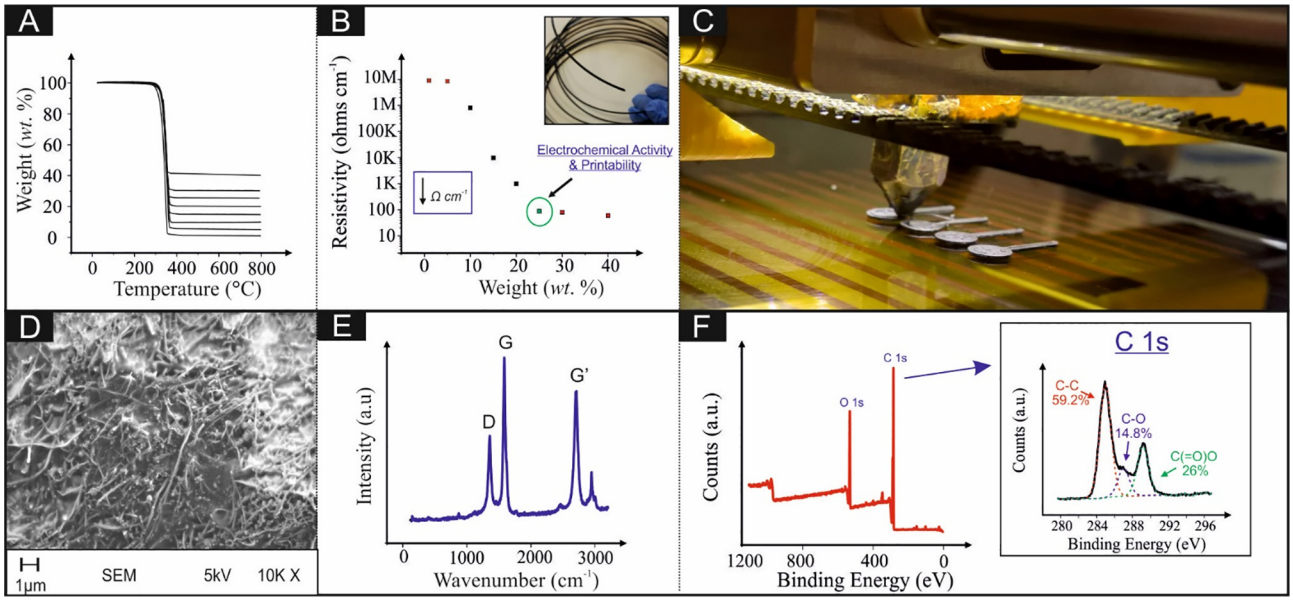

Fig. 1. Physicochemical characterisation of the NG/PLA filaments and AMEs. A: Thermogravimetric analysis, B: Resistivity *vs.* NG content, C: AM process of the AMEs (for electrochemical characterisation), D: SEM analysis of 25 wt% NG/PLA, E and F: Raman and XPS analysis of the AMEs.

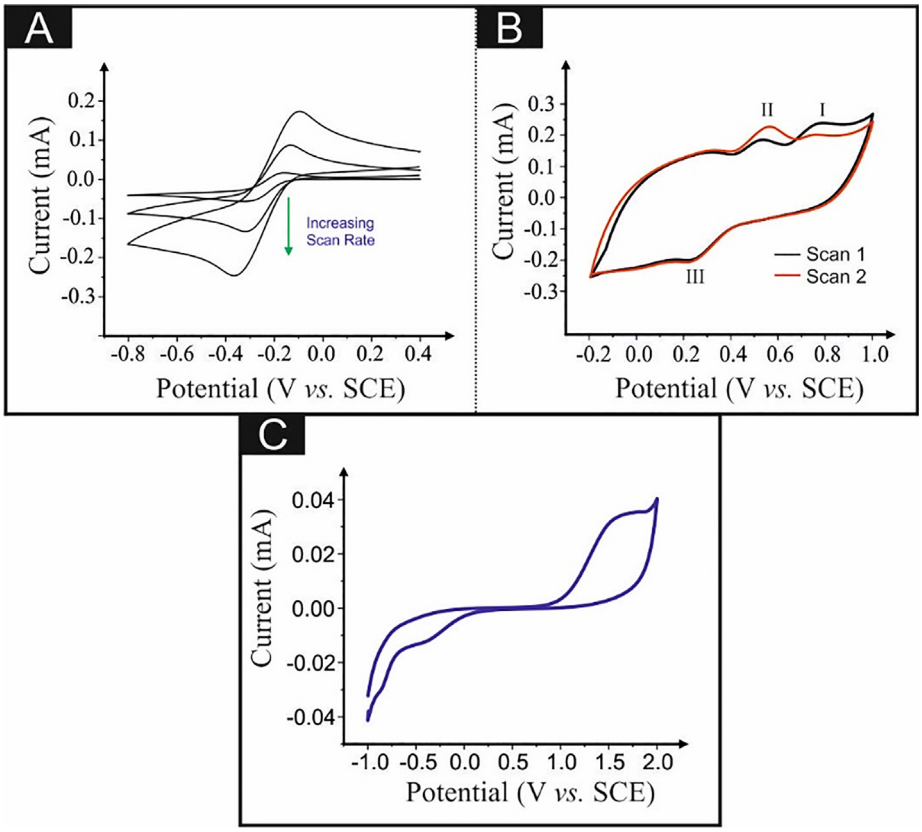

Fig. 2. Electrochemical characterisation of the AMEs, using (A) 1 mM hexammineruthenium (III) in 0.1 M KCl at varying scan rates (5, 100 & 200 mV s^{-1}), (B) 1 mM capsaicin in 0.1 M $HClO_4$; Scan rate 50 mV s^{-1} and (C) ammonium iron (II) sulfate in 0.2 M $HClO_4$; Scan rate: 50 mV s^{-1}.

subjected to an anodic process occurring at ~ +0.53 V (peak II).

The electrochemical response using the AMEs appears to be mechanistically similar to that observed graphitic electrodes, which is expected [13,14]. Fig. 2C depicts the cyclic voltammetric response towards 1 mM ammonium iron (II) sulfate, which known to be very sensitive to oxygenated species residing on the electrode surface. This probe has been reported by Chen *et al.* [12] and Cumba *et al.* [15] to dramatically decrease the peak-to-peak separation observed upon an increase in oxygenated groups [12,15], giving insight into surface oxygen species analysis of the cyclic voltammogram utilising AMEs demonstrates a peak-to-peak separation of ~1.0 V. Such a peak-to-peak large separation indicates that the oxygen species (C-O and C(=O)O groups) determined above by the XPS analysis, are from the PLA structure rather than oxygenated graphite otherwise a lower peak-to-peak seperation would be observed [12,15]. The electrochemical activity (utilising both outer and inner-sphere redox probes) of these AMEs demonstrate their suitability and possible application as electrochemical sensing devices.

Next, the AMEs are towards the electrochemical sensing of lead (II) and cadmium (II). Fig. 3 depicts typical square-wave voltammograms (SWV) using AMEs and their corresponding calibration plots for the simultaneous sensing of lead (II) and cadmium (II) utilising the AMEs (Fig. 3A). It is clear from Fig. 3A that the AMEs demonstrate typical metallic stripping behaviour, for the simultaneous detection of lead (II) and cadmium (II). Analysis of the SWV profiles in the form of plots of peak height (I_p) *vs.* concentration are found to be linear over the concentration range with the following linear regressions: I_p (μA) = 20 μA/ mg L^{-1} – 10 μA; R^2 = 0.98; (N = 11) and I_p (μA) = 10 μA/ mg L^{-1} – 4 μA; R^2 = 0.99; (N = 11) for lead (II) and cadmium (II), respectively. However, it is clear that the lowest linear range (0.19–4.5 mg L^{-1} and 0.79–4.5 mg L^{-1} for lead (II) and cadmium (II), respectively) and detection limit (lead (II) = 0.16 mg L^{-1} and cadmium (II) = 0.32 mg L^{-1}, is much larger than that of the levels set by the World Health Organisation (WHO) corresponding to 10.0 μg L^{-1} and 3.0 μg L^{-1} for lead (II) and cadmium (II), respectively. In an attempt to increase the sensitivity of the AMEs, an AM large surface-area honeycomb structure (see Fig. 3B) was fabricated and explored towards the sensing of lead (II) and cadmium (II). Analysis of the SWV profiles in the form of plots of I_p *vs.* concentration are found to be linear over the concentration range with the following linear regressions: I_p (μA) = 100 μA/ mg L^{-1} – 10 μA; R^2 = 0.98; (N = 11) and I_p (μA) = 40 μA/ mg L^{-1} – 20 μA; R^2 = 0.97; (N = 11) for lead (II) and cadmium (II), respectively. It is clear that the large surface AM electrode design does increase the sensitivity for the detection of cadmium (II), however these still do not meet the required standards set by the WHO. Recently, Dos Santos *et al.* [8], have electrochemically pre-treated an AME with an oxidation at +1.8 V (*vs.* SCE), followed by reduction from 0 to −1.8 V, exhibiting an increase within the electron transfer kinetics due to the exposure of graphene sheets on the surface of the electrode and the presence of oxygen functionalities increased the interaction with dopamine [8]. Inspired by such reports, we investigated the effect of electrochemical pre-treatment upon the electrode surface by simulating the pre-treatment method presented by Dos Santos *et al.* [8] However, this had no measurable effect upon the electroanalytical response of the sensors, due to the fact that the electrochemical method involves an electrochemical pre-treatment step already as a part of the SWV methodology hence, *additional* electrochemical pre-treatment offers no further benefit.

The ability to AM electrochemical configurations does allow for the mass-production of freestanding, complex 3D structures that other printing/manufacturing routes cannot achieve. However, we next consider the response of the AM electrochemical sensing platform to that of extensively utilised screen-printed electrode (SPE) sensors. SPEs offer a low-cost and portable electrode platform that due to their

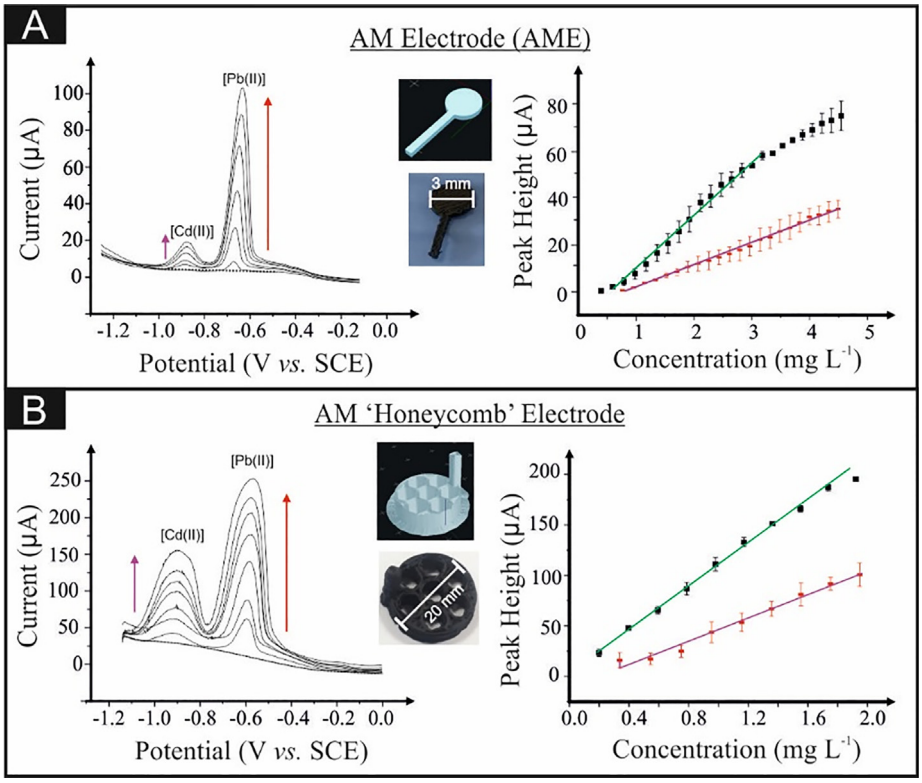

Fig. 3. Square-wave voltammograms and corresponding calibration plots ($N = 11$) for the simultaneous detection of lead (II) (black squares) and cadmium (II) (red squares) (within pH 2 0.1 M HCl) utilising a 3 mm diameter AME (A) and an AM large surface area 'honeycomb' 20 mm diameter × 5 mm height electrode (B).

economy-of-scales provide the basis of the multi-billion dollar glucose sensing market, and have been routinely applied within an array of electrochemical applications. Upon consultation of our previous work [16], the limit-of-detections (LOD) of lead (II) and cadmium (II), using 3 mm diameter graphitic SPEs are 2.0 and 2.2 μg L^{-1}, respectively. Such vast variation within the LOD is strange considering the electrochemical performance provided by the previously mentioned, electrochemical characterisation using an outer-sphere redox probe (1 mM hexaammineruthenium (III) chloride), which is in good agreement with typically used graphitic based SPEs (*i.e.* 10^{-3} cm s^{-1}). The difference observed towards the sensing of lead (II) and cadmium (II) is due to the fact that the redox probe is conducted at 1 mM, while the sensing of lead (II) and cadmium (II) is very low. In the latter case the capacitive currents, as noted earlier, limits their electroanalytical utilisation. Note that this paper provides for the first time the highest reported NG-loaded *wt.* % filaments, which exhibit good printability but yet the overall loading is still too low to be comparable to electrochemical sensors (*i.e.* SPEs). This is expected as the AMEs are ~75 wt% plastic and only possess ~25 wt% of electrochemically active material; further work is currently underway to improve their electroanalytical capabilities.

3. Conclusions

Herein, we have reported for the first time, the fabrication, characterisation (physicochemical and electrochemical) and implementation (electrochemical sensing) tailorable and controllable nanographite (NG) loaded PLA additive manufacturable (printable) filaments. Note that this is the highest-loaded filaments reported to date, but yet are printable. Proof-of-concept is shown towards the sensing of lead (II) and cadmium (II). We note that while these AM electrochemical sensors are not able to reach WHO levels, it must be reminded that the electrode is comprised of 75% plastic and only 25% active material. The limitation of this approach is the limit on the active material while still being printable however, the benefits of this approach are evident allowing economical electrochemical devices to be fabricated with structures that cannot be made easily by traditional manufacturing (*i.e.* honeycomb structures). Future work is consequently directed towards improving the electrochemical performance of these AM devices through increasing the % of active material

4. Methods

All chemicals used were obtained from Sigma-Aldrich at an analytical grade and were used without any further purification. All solutions were prepared with deionised water of resistivity not less than 18.2 MΩ cm. Voltammetric measurements were carried out using an Autolab PGSTAT100 (Metrohm, The Netherlands) potentiostat.

Nanographite (NG) / PLA filaments were fabricated by pre-mixing NG (mesoporous nanopowder less than 500 nm particle size a (DLS) > 99.95% trace metal basis, Sigma Aldrich, UK) and PLA utilising a facile solution based mixing step, briefly the NG was dispersed within xylene and heated (under reflux) at 160 °C for 3 h, the PLA was then added to the mixture and left for a further 3 h. The resulting homogenous (solution phase) mixture then was then recrystallized within methanol, and left to dry (at 50 °C within a fan oven) until the xylene had evaporated. The resulting NG/PLA *powder* was then placed within a MiniCTW twin-screw extruder (ThermoScientific) at a temperature of 200 °C and a screw speed of 30 rpm, the diameter (1.75 mm) of the filament was controlled with a specific die with a set diameter. The 3D printed designs were fabricated using a ZMorph® printer (Warsaw, Poland) with a direct drive extruder at a temperature of 190 °C, 60 °C bed, 0.2 mm layer height, Rectilinear infill, 0.4 mm nozzle; travel speed is the zmorph default of 120 mm/s.

The potentiostatic electrochemical experiments were carried out utilising a three-electrode setup with either the NG/PLA AM electrode (AME) as the working electrode (with a diameter of 3 mm and a thickness of 1 mm), an SCE and nickel as the reference and counter

electrodes, respectively. Each AME for these electrochemical characterisation experiments were printed with a connecting strip allowing simple connection to a crocodile clip [17].

Scanning electron microscope (SEM) images and surface element analysis were obtained with a JEOL JSM-5600LV model equipped with an energy-dispersive X-ray (EDX) microanalysis package. Raman spectroscopy was performed using a Renishaw InVia spectrometer with a confocal microscope (×50 objective) spectrometer with an argon laser (514.3 nm excitation) at a very low laser power level (0.8 mW) to avoid any heating effects. Thermogravimetric analysis (TGA) was conducted utilising a PerkinElmer TGA 4000. The PLA samples were subject to a gradual temperature increase of 10 °C per minute, over a range between 25 and 800 °C, under a flow of nitrogen (40 mL/min). The X-ray photoelectron spectroscopy (XPS) data was acquired using a bespoke ultra-high vacuum system fitted with a Specs GmbH Focus 500 monochromated Al Kα X-ray source, Specs GmbH Phoibos 150 mm mean radius hemispherical analyser with 9-channeltron detection, and a Specs GmbH FG20 charge neutralising electron gun. Survey spectra were acquired over the binding energy range 1100 – 0 eV using a pass energy of 50 eV and high-resolution scans were made over the C 1s and O 1s lines using a pass energy of 20 eV. Under these conditions the full width at half maximum of the Ag $3d_{5/2}$ reference line is ~0.7 eV. In each case, the analysis was an area-average over a region approximately 1.4 mm in diameter on the sample surface, using the 7 mm diameter aperture and lens magnification of ×5. The energy scale of the instrument is calibrated according to ISO 15472, and the intensity scale is calibrated using an in-house method traceable to the UK National Physical Laboratory. Data was quantified using Scofield cross sections corrected for the energy dependencies of the electron attenuation lengths and the instrument transmission. Data interpretation was carried out using CasaXPS software v2.3.16.

The heterogeneous electron transfer rate constant, k^0_{obs}, were determined utilising the Nicholson method through the use of the following equation: $\psi = k^0_{obs}[\pi D n\nu F/(RT)]^{-1/2}$ where ψ is the kinetic parameter, D is the diffusion coefficient, n is the number of electrons involved in the process, F is the Faraday constant, R is the universal gas constant and T is the temperature [18]. The kinetic parameter, ψ, is tabulated as a function of ΔE_P (peak-to-peak separation) at a set temperature (298 K) for a one-step, one electron process with a transfer coefficient, α, equal to 0.5. The function of ψ (ΔE_P), which fits Nicholson's data, for practical usage (rather than producing a working curve) is given by: $\psi = (-0.6288 + 0.0021X)/(1–0.017X)$ where $X = \Delta E_P$ is used to determine ψ as a function of ΔE_P from the experimentally recorded voltammetry; from this, a plot of ψ against $[\pi D n\nu F/(RT)]^{-1/2}$ allows the k^0_{obs} to be readily determined [19]. The heterogeneous electron transfer rate constants were calculated assuming a diffusion coefficient of 9.10×10^{-6} cm^2 s^{-1} for hexaammineruthenium (III) chloride [20]. Electrochemical analysis of the lead (II) and cadmium (II) was carried out utilising the peak currents (or heights) from an extrapolated baseline current.

Acknowledgments

Funding from the Engineering and Physical Sciences Research Council (Reference: EP/N001877/1) is acknowledged.

Contributions

C.E.B conceived the concept. C.W.F and C.E.B designed the experiments. M.P.D and E.M.K created and designed the 3D models. H.M.E carried out the electrochemical procedures. C.W.F undertook the polymer related experiments and AM / 3D printing. C.W.F and C.E.B performed data analysis. G.C.S performed the XPS and its analysis. C.W.F and C.E.B wrote the manuscript, and all the authors discussed the results, contributed to the draft of the manuscript and commented on the final version. C.E.B coordinated the overall project.

Declaration of Competing Interest

The authors declare no competing interests.

References

[1] C.W. Foster, M.P. Down, Y. Zhang, X. Ji, S.J. Rowley-Neale, G.C. Smith, P.J. Kelly, C.E. Banks, 3D Printed Graphene Based Energy Storage Devices, Sci. Rep. 7 (2017) 42233.
[2] Z. Rymansaib, P. Iravani, E. Emslie, M. Medvidović-Kosanović, M. Sak-Bosnar, R. Verdejo, F. Marken, All-Polystyrene 3D-Printed Electrochemical Device with Embedded Carbon Nanofiber-Graphite-Polystyrene Composite Conductor, Electroanalysis 28 (7) (2016) 1517–1523.
[3] A. Ambrosi, M. Pumera, 3D-printing technologies for electrochemical applications, Chem. Soc. Rev. 45 (10) (2016) 2740–2755.
[4] B.R. Liyarita, A. Ambrosi, M. Pumera, 3D-printed Electrodes for Sensing of Biologically Active Molecules, Electroanalysis 30 (7) (2018) 1319–1326.
[5] C. Tan, M.Z.M. Nasir, A. Ambrosi, M. Pumera, 3D Printed Electrodes for Detection of Nitroaromatic Explosives and Nerve Agents, Anal. Chem. 89 (17) (2017) 8995–9001.
[6] A.L. Silva, M.M. Correa, G.C. de Oliveira, R.C. Michel, F.S. Semaan, E.A. Ponzio, Development and application of a routine robust graphite/poly(lactic acid) composite electrode for the fast simultaneous determination of Pb2+ and Cd2+ in bijou by square wave anodic stripping voltammetry, New J. Chem. (2018).
[7] X. Wei, D. Li, W. Jiang, Z. Gu, X. Wang, Z. Zhang, Z. Sun, 3D Printable Graphene Composite, Sci. Rep. 5 (2015) 11181.
[8] P.L. dos Santos, V. Katic, H.C. Loureiro, M.F. dos Santos, D.P. dos Santos, A.L.B. Formiga, J.A. Bonacin, Enhanced performance of 3D printed graphene electrodes after electrochemical pre-treatment: Role of exposed graphene sheets, Sens. Actuators, B 281 (2019) 837–848.
[9] M.A. Pimenta, G. Dresselhaus, M.S. Dresselhaus, L.G. Cançado, A. Jorio, R. Saito, Studying disorder in graphite-based systems by Raman spectroscopy, PCCP 9 (11) (2007) 1276–1290.
[10] A. García-Miranda Ferrari, C. Foster, P. Kelly, D. Brownson, C. Banks, Determination of the Electrochemical Area of Screen-Printed Electrochemical Sensing Platforms, Biosensors 8 (2) (2018) 53.
[11] X. Ji, C.E. Banks, A. Crossley, R.G. Compton, Oxygenated Edge Plane Sites Slow the Electron Transfer of the Ferro-/Ferricyanide Redox Couple at Graphite Electrodes, ChemPhysChem 7 (6) (2006) 1337–1344.
[12] P. Chen, R.L. McCreery, Control of Electron Transfer Kinetics at Glassy Carbon Electrodes by Specific Surface Modification, Anal. Chem. 68 (22) (1996) 3958–3965.
[13] E. Blanco, C.W. Foster, L.R. Cumba, D.R. do Carmo, C.E. Banks, Can solvent induced surface modifications applied to screen-printed platforms enhance their electroanalytical performance? Analyst 141 (9) (2016) 2783–2790.
[14] E.P. Randviir, J.P. Metters, J. Stainton, C.E. Banks, Electrochemical impedance spectroscopy versus cyclic voltammetry for the electroanalytical sensing of capsaicin utilising screen printed carbon nanotube electrodes, Analyst 138 (10) (2013) 2970–2981.
[15] L.R. Cumba, C.W. Foster, D.A.C. Brownson, J.P. Smith, J. Iniesta, B. Thakur, D.R. do Carmo, C.E. Banks, Can the mechanical activation (polishing) of screen-printed electrodes enhance their electroanalytical response? Analyst 141 (9) (2016) 2791–2799.
[16] C.W. Foster, A.P. de Souza, J.P. Metters, M. Bertotti, C.E. Banks, Metallic modified (bismuth, antimony, tin and combinations thereof) film carbon electrodes, Analyst 140 (22) (2015) 7598–7612.
[17] F.E. Galdino, C.W. Foster, J.A. Bonacin, C.E. Banks, Exploring the electrical wiring of screen-printed configurations utilised in electroanalysis, Anal. Methods 7 (3) (2015) 1208–1214.
[18] R.S. Nicholson, Theory and Application of Cyclic Voltammetry for Measurement of Electrode Reaction Kinetics, Anal. Chem. 37 (11) (1965) 1351–1355.
[19] I. Lavagnini, R. Antiochia, F. Magno, An Extended Method for the Practical Evaluation of the Standard Rate Constant from Cyclic Voltammetric Data, Electroanalysis 16 (6) (2004) 505–506.
[20] C.E. Banks, R.G. Compton, A.C. Fisher, I.E. Henley, The transport limited currents at insonated electrodes, PCCP 6 (12) (2004) 3147–3152.